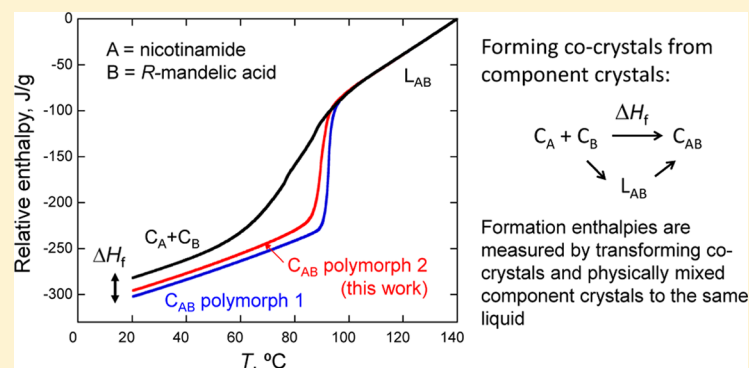


Formation Enthalpies and Polymorphs of Nicotinamide–*R*-Mandelic Acid Co-CrystalsSi-Wei Zhang,<sup>†</sup> Ilia A. Guzei,<sup>†</sup> Melgardt M. de Villiers,<sup>†</sup> Lian Yu,<sup>†,\*</sup> and Joseph F. Krzyzaniak<sup>‡</sup><sup>†</sup>School of Pharmacy and Department of Chemistry, University of Wisconsin—Madison, Madison, Wisconsin 53705, United States<sup>‡</sup>Pfizer Global Research & Development, Groton, Connecticut 06340, United States

## Supporting Information



**ABSTRACT:** Co-crystals provide an opportunity to improve the properties of pharmaceuticals and other materials. We report a method for determining the formation enthalpies of co-crystals in which enthalpies of melting are measured for a co-crystal and the physical mixture of its component crystals. Because the two melting processes arrive at the same liquid, the difference of their enthalpy changes is the co-crystal's formation enthalpy. For the system of nicotinamide (NIC) and *R*-mandelic acid (RMA), the formation enthalpy at 30 °C is  $-23$  (3) J/g for polymorph 1 and  $-18$  (3) J/g for polymorph 2. These values are comparable with the enthalpy of mixing for NIC and RMA liquids [ $-49$  (4) J/g at 160 °C], indicating the need for correcting for nonideal mixing in calculating formation enthalpies of co-crystals via thermodynamic cycles. This correction is made automatically in our method by performing measurements with physical mixtures of component crystals, as opposed to pure component crystals. One of the NIC-RMA polymorphs (2) was discovered in this work, and its structure and thermodynamic relation to polymorph 1 are reported.

## INTRODUCTION

A co-crystal is a solid phase that contains multiple chemical components.<sup>1</sup> The existence of co-crystals has been known for a long time, under the name “compound” for fixed stoichiometry and “solid solution” for variable stoichiometry. A racemic compound is a co-crystal of two opposite enantiomers (resolvable chiral molecules).<sup>2</sup> Interest in co-crystals has increased in recent years, driven in part by their applications in improving the properties of pharmaceutical solids,<sup>3–8</sup> including solubility,<sup>5</sup> bioavailability,<sup>6</sup> and mechanical properties.<sup>8</sup>

Many studies have examined the discovery, structure, and formation of co-crystals, while the work has been limited on the thermodynamics of co-crystals. Little data exist, for example, on the enthalpy and free energy of formation of co-crystals,<sup>9,10</sup> which are fundamental measures of their stability. The formation properties are defined in reference to the following reaction:



where  $C_A$ ,  $C_B$ , and  $C_{AB}$  are the crystal of component A, the crystal of component B, and the co-crystal of A and B, respectively. The enthalpy of formation  $\Delta H_f$  is the enthalpy (or effectively energy at ambient pressure) of the co-crystal relative to its component crystals; the free energy of formation  $\Delta G_f$  measures the thermodynamic stability of the co-crystal relative to the component crystals, with the entropy effect included.  $\Delta H_f$  and  $\Delta G_f$  are valuable data for understanding co-crystallization. For example, the formation properties for a series of co-crystals in which components are systematically varied help understand the molecular factors that influence the stability of co-crystals. One aim of this study was to test a general method for measuring formation enthalpies of co-crystals.

A question concerning co-crystallization is whether multi-component crystals are less likely polymorphic than single-component crystals.<sup>11</sup> Besides a fundamental interest in

Received: April 27, 2012

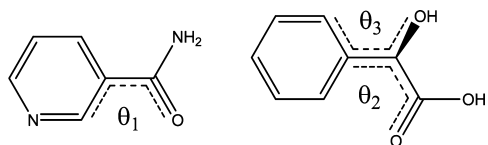
Revised: July 3, 2012

Published: July 6, 2012

answering this question, the fact that many co-crystals are polymorphic<sup>12–16</sup> requires that the study of co-crystals takes into account the discovery and control of co-crystal polymorphs.

The co-crystallization of nicotinamide (NIC) and *R*-mandelic acid (RMA) (Scheme 1) has been studied by Frišić and

**Scheme 1. Structures of Nicotinamide (NIC) and *R*-Mandelic Acid (RMA)<sup>a</sup>**



Nicotinamide (NIC)    *R*-mandelic acid (RMA)

<sup>a</sup> $\theta_1$ ,  $\theta_2$ , and  $\theta_3$  indicate angles of torsion.

Jones.<sup>17</sup> NIC (Vitamin B<sub>3</sub>) is a generally recognized as safe (GRAS) substance useful as solubility enhancer<sup>18</sup> and co-crystal former.<sup>13,17,19–21</sup> Besides RMA, NIC can co-crystallize with many other carboxylic acids.<sup>17,19,20</sup>

We report here a new polymorph of the NIC-RMA co-crystal, which is thermodynamically less stable than the known structure.<sup>17</sup> We also report the formation enthalpies for the two polymorphs measured with a method implemented in this work. For the NIC-RMA system, the enthalpy of mixing in the liquid state is substantial and correction for this effect is needed in calculating the co-crystals' formation enthalpies via thermodynamic cycles. Our method automatically makes this correction, by making measurements with a physical mixture of component crystals, as opposed to the pure component crystals.

## ■ DETERMINATION OF FORMATION ENTHALPIES OF CO-CRYSTALS

In this section, we describe a method for determining the formation enthalpies of co-crystals and compare it with other procedures for this purpose. This method relies on the fact that the co-crystal  $C_{AB}$  and the physical mixture of component crystals ( $C_A + C_B$ ) (the two sides of eq 1) have the same liquid upon melting or the same solution upon dissolution. Thus, the formation enthalpy of  $C_{AB}$  can be calculated from the relevant enthalpies of melting or dissolution as follows:

$$\Delta H_f = \Delta H_{m(A+B)}(T_S \rightarrow T_L) - \Delta H_{mAB}(T_S \rightarrow T_L) \quad (2)$$

$$\Delta H_f = \Delta H_{s(A+B)}(T_S) - \Delta H_{sAB}(T_S) \quad (3)$$

In eq 2,  $T_S$  is a temperature at which  $C_{AB}$  and ( $C_A + C_B$ ) are solid and at which  $\Delta H_f$  is to be evaluated,  $T_L$  is a temperature at which  $C_{AB}$  and ( $C_A + C_B$ ) are both melted, and  $\Delta H_{m(A+B)}(T_S \rightarrow T_L)$  and  $\Delta H_{mAB}(T_S \rightarrow T_L)$  are the corresponding changes in enthalpy, with ( $T_S \rightarrow T_L$ ) signifying that  $\Delta H_m$  is measured cumulatively from  $T_S$  to  $T_L$ . In eq 3,  $\Delta H_{sAB}(T_S)$  and  $\Delta H_{s(A+B)}(T_S)$  are the enthalpies of solution for  $C_{AB}$  and ( $C_A + C_B$ ) in the same solvent to the same concentration at  $T_S$ .

The validity of eqs 2 and 3 is clear from the thermodynamic principle that the enthalpy change of a given reaction can be obtained by summing the enthalpy changes along different paths that connect the initial to the final state. Equations 2 and 3 correspond to two different paths from ( $C_A + C_B$ ) to  $C_{AB}$ , involving melting and dissolution, respectively. Still other paths

can be imagined that complete eq 1; for example, paths that involve evaporation or combustion. In practice, temperature-scanning calorimeters can yield the enthalpies of melting needed in eq 2, as we demonstrate in this work, and isothermal calorimeters the enthalpies of solution in eq 3.

The key point of our proposed method is not the possibility to measure the formation enthalpies of co-crystals in different ways, but the advantage of performing measurements on the *physical mixture* ( $C_A + C_B$ ), as opposed to the pure component crystals  $C_A$  and  $C_B$ , in achieving this goal, which we now explain. If the enthalpy of mixing for components A and B in the liquid state is negligible,  $\Delta H_{m(A+B)}$  and  $\Delta H_{s(A+B)}$  in eqs 2 and 3 are the sums of the corresponding enthalpies for the pure component crystals (properly weighted to ensure mass balance), yielding

$$\Delta H_f = \Delta H_{mA}(T_S \rightarrow T_L) + \Delta H_{mB}(T_S \rightarrow T_L) - \Delta H_{mAB}(T_S \rightarrow T_L) \quad (4)$$

$$\Delta H_f = \Delta H_{sA}(T_S) + \Delta H_{sB}(T_S) - \Delta H_{sAB}(T_S) \quad (5)$$

Here  $\Delta H_{mA}$ ,  $\Delta H_{mB}$ , and  $\Delta H_{mAB}$  are the enthalpies of melting of  $C_A$ ,  $C_B$ , and  $C_{AB}$ ;  $\Delta H_{sA}$ ,  $\Delta H_{sB}$ , and  $\Delta H_{sAB}$  are the corresponding heats of solution. Thus, instead of measuring the *physical mixture* ( $C_A + C_B$ ), one can measure the pure component crystals  $C_A$  and  $C_B$  separately and calculate  $\Delta H_f$  via eqs 4 and 5. This method has been used to calculate the formation enthalpies of racemic compounds (special co-crystals in which A and B are the opposite enantiomers)<sup>2,22</sup> and some other co-crystals,<sup>10</sup> but it is important to note the assumption of ideal mixing that leads to eqs 4 and 5.

For racemic compounds, the assumption of ideal mixing has been justified on the ground that except for different handedness, opposite enantiomers are chemically identical (if one is an acid, for example, so is the other), such that their mixing in the liquid state is similar to "mixing" the same molecules with  $\Delta H_{mix} \approx 0$ .<sup>2</sup> In contrast, ideal mixing is not justified for two arbitrary components that co-crystallize. It is common that acid-like and base-like components combine to form co-crystals, for which the heat of component mixing is likely significant, and found to be so for the system carbamazepine-saccharin.<sup>9</sup>

To account for nonideal mixing, Oliveira et al. measured the dissolution of component crystals not in a pure solvent but one containing the second component<sup>9</sup> such that the final solution is the same as that formed by dissolving the co-crystal  $C_{AB}$ . Their procedure is thermodynamically equivalent to ours. In their procedure, two measurements were performed to yield the enthalpy of dissolving  $C_A$  in a solvent that contains B,  $\Delta H_{sA(B)}$ , and the enthalpy of dissolving  $C_B$  in the solvent that contains A,  $\Delta H_{sB(A)}$ , and the sum [ $\Delta H_{sA(B)} + \Delta H_{sB(A)}$ ] was calculated. It is evident that the latter sum is the same as  $\Delta H_{s(A+B)}$  in eq 3, which in our proposal, would be measured in a single dissolution experiment of the physical mixture ( $C_A + C_B$ ) in the pure solvent. Thus, as long as the physical mixture is stable against conversion to the co-crystal before testing, our method would require one fewer measurement.

## ■ METHODS

*R*-Mandelic acids (RMA) and nicotinamide (NIC, the stable polymorph<sup>23</sup>) were purchased from Sigma-Aldrich (St. Louis, MO, USA) and used as received. Anhydrous acetonitrile (Fisher Scientific, Pittsburgh, PA, USA) was of the HPLC grade.

Powder X-ray diffraction was performed with a Bruker D8 Advance diffractometer (Cu  $K\alpha$  radiation, voltage 40 kV, and current 40 mA). Approximately 5 mg of powder was sprinkled on the surface of a zero-

background silicon (510) sample holder and scanned from  $2^\circ$  to  $40^\circ$   $2\theta$  at a speed of  $1.2^\circ/\text{min}$  and a step size of  $0.02^\circ$ . Hot-stage microscopy was performed with a Linkam THMS 600 hot-stage and an Olympus BH2-UMA light microscope equipped with a digital camera. Raman microscopy was performed with a Thermo Scientific DXR Raman microscope and a 10 mW 532 nm laser and was used to distinguish crystal polymorphs.

Differential scanning calorimetry (DSC) was conducted in Tzero aluminum pans using a TA Instruments Q2000 unit under 50 mL/min  $\text{N}_2$  purge. In a typical measurement, 5–10 mg of sample was heated at  $20^\circ\text{C}/\text{min}$  to  $160^\circ\text{C}$  to measure the temperature and heat of melting, cooled at  $20^\circ\text{C}/\text{min}$ , and heated again at  $10^\circ\text{C}/\text{min}$  to record the glass transition temperature of the melt.

Frišćić and Jones prepared a co-crystal of NIC and RMA (hereafter polymorph 1) by liquid-assisted grinding.<sup>17</sup> In this study, polymorph 1 was also obtained by crystallizing a supercooled liquid of NIC and RMA in 1:1 molar ratio. In this preparation, a liquid film (3 mg) was formed between two coverslips by melting at  $100^\circ\text{C}$  and cooling to  $25^\circ\text{C}$ . The liquid crystallized spontaneously at  $25^\circ\text{C}$  in 4 days, and the product was found to be polymorph 1 by X-ray diffraction. Polymorph 1 was also obtained by solution crystallization with seeding. For this purpose, a 2 mL acetonitrile (ACN) solution of NIC and RMA (both at 1 M) was prepared at  $60^\circ\text{C}$ , filtered through a  $5\ \mu\text{m}$  syringe filter, and seeded at room temperature. The resulting crystals were filtered, washed with ACN, and dried in vacuum.

A second polymorph (polymorph 2) of the NIC-RMA co-crystal was discovered by crystallizing an ACN solution of NIC and RMA at a 1:1 molar ratio. The solution was evaporated at  $25^\circ\text{C}$  to form a thick transparent liquid and evacuated to dryness. The resulting crystals showed a different X-ray diffraction pattern from polymorph 1. Later, higher-quality crystals of polymorph 2 were precipitated from solution by seeding. For this purpose, the same procedure described above for the seeded crystallization of polymorph 1 was employed, except with seeds of polymorph 2.

To prepare a physical mixture of NIC and RMA crystals, each material was passed through a sieve with  $250\ \mu\text{m}$  openings. The sieved powders were mixed in 1:1 molar ratio with a vortex mixer (Vortex Genie K-550-G Mixer) at the maximum speed for 1 min. The final mixture was analyzed by X-ray diffraction to ensure that it contained only component crystals and no co-crystals and used immediately for subsequent DSC analysis.

Single-crystal X-ray diffraction evaluation and data collection were performed at 100 K on a Bruker SMART APEXII diffractometer with  $\text{Cu K}\alpha$  ( $\lambda = 1.54178\ \text{\AA}$ ) radiation, and the crystal structure was solved using a standard procedure (see Supporting Information for details).

## RESULTS AND DISCUSSION

**Polymorphs of NIC-RMA Co-Crystals.** Our crystallization experiments reproduced the co-crystal of Frišćić and Jones<sup>17</sup> and found a new polymorph. The XRD pattern of the new polymorph differs from that of the known polymorph (Figure 1) and those of the component crystals (not shown). Single crystals of the new polymorph were grown from a seeded ACN solution and used for structural solution by X-ray diffraction (Table 1). The XRD pattern simulated from the single-crystal structure matches well with the powder XRD pattern of the new polymorph (Figure 1). Hereafter we refer to the new polymorph as “polymorph 2” and the previous polymorph “polymorph 1”.

Table 1 compares the structures of the two polymorphs of NIC-RMA co-crystals. Polymorph 1 is monoclinic (space group  $C2$ ) with two symmetry-independent RMA molecules and two symmetry-independent NIC molecules.<sup>17</sup> Polymorph 2 is monoclinic (space group  $P2_1$ ) with one each symmetry-independent molecule of NIC and RMA. Polymorph 1 is slightly denser than polymorph 2, even at a higher temperature.

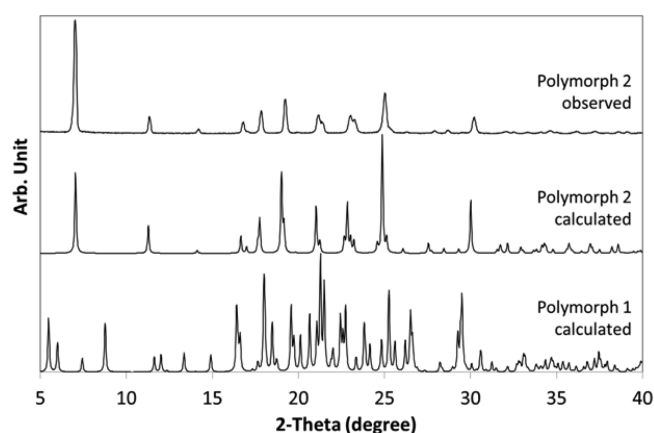


**Figure 1.** XRD patterns of NIC-RMA co-crystals. Bottom: Polymorph 1 (CSD: JILZOU).<sup>17</sup> Top: Polymorph 2 (this work). Middle: Simulated pattern from the crystal structure of polymorph 2 (Table 1).

**Table 1.** Crystal Structures of NIC-RMA Co-Crystals<sup>a</sup>

	polymorph	
	1 (JILZOU) <sup>17</sup>	2
<i>T</i> , K	150(2)	100(1)
wavelength, $\text{\AA}$	0.71073	1.54178
crystal system	monoclinic	monoclinic
space group	$C2$	$P2_1$
description	needle	plate
crystal size, $\text{mm}^3$	$0.46 \times 0.07 \times 0.07$	$0.28 \times 0.18 \times 0.16$
<i>a</i> , $\text{\AA}$	32.6557(9)	5.2406(3)
<i>b</i> , $\text{\AA}$	5.475(1)	10.0477(6)
<i>c</i> , $\text{\AA}$	14.9264(5)	12.6006(7)
$\beta$ , deg	99.400(1)	95.678(4)
volume, $\text{\AA}^3$	2632.9(5)	660.24(7)
<i>Z</i>	8	2
$\rho$ , $\text{g cm}^{-3}$	1.384	1.380
$\mu$ , $\text{mm}^{-1}$	0.103	0.857
<i>F</i> (000)	1152	288
$\theta$ range, deg	3.77–27.43	3.52–67.60
data/restraints/parameters	5773/1/361	1235/1/183
<i>S</i>	1.12	1.011
<i>R</i> <sub>1</sub>	0.055	0.0430
w <i>R</i> <sub>2</sub> for [ <i>I</i> > 2 $\sigma$ ( <i>I</i> )]	0.128	0.1138
<i>R</i> <sub>1</sub>	0.070	0.0472
w <i>R</i> <sub>2</sub> for all data	0.138	0.1174
$\Delta$ , $\text{e \AA}^{-3}$ , min, max	−0.295, 0.293	−0.248, 0.306

<sup>a</sup>Molecular formula:  $\text{C}_{14}\text{H}_{14}\text{N}_2\text{O}_4$ . Molecular weight: 274.27 g/mol.

To evaluate their structural difference, we calculated the radial distribution functions (RDF) of molecular centers of mass for both polymorphs (Figure 2). The RDF is one descriptor of the local molecular environment in a crystal. The RDF is to be calculated for each symmetry-independent molecule and each chemical component in a co-crystal. Thus, NIC-RMA polymorph 2 has three distinct RDFs (Figure 2): NIC-NIC, which reports the distribution of NIC molecules around an NIC molecule; RMA-RMA, the distribution of RMA molecules around an RMA molecule; and NIC-RMA, the distribution of RMA molecules around an NIC molecule (or equivalently, NIC molecules around an RMA molecule). For polymorph 1, there are more unique RDFs owing to its symmetry-independent molecules. For simplicity, Figure 2 displays only the *average* RDFs for the NIC and RMA

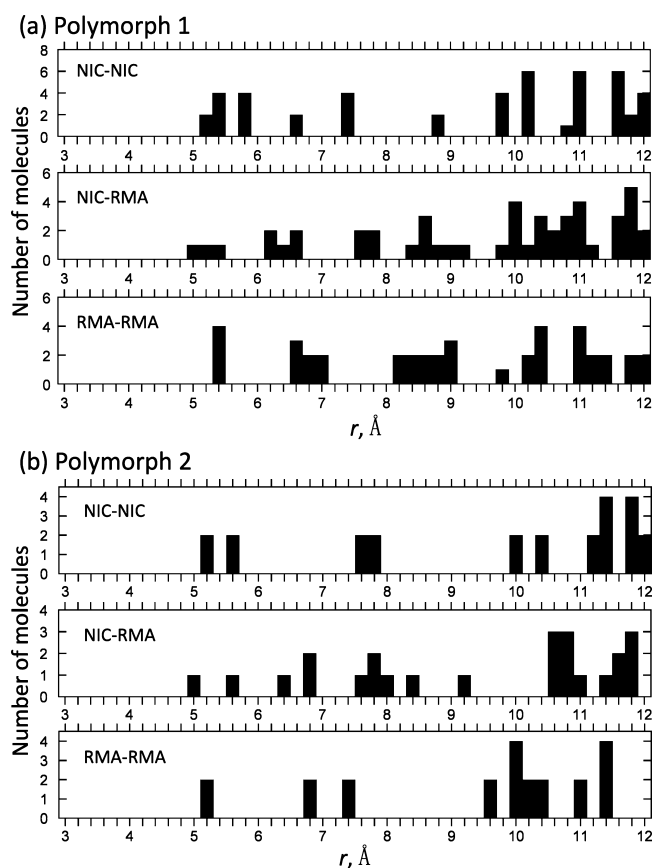


**Figure 2.** Radial distribution functions (RDF) of molecular centers of mass in polymorphs 1 and 2 of NIC-RMA co-crystals.

molecules in polymorph 1; the individual RDFs are reasonably similar for the symmetry-independent molecules of NIC and RMA.

The RDF analysis shows that for every molecule in an NIC-RMA co-crystal, the nearest molecular neighbor is approximately 5 Å away. The spatial distributions of molecules in the two polymorphs are significantly different. Within the first 10 Å, the NIC–NIC and RMA–RMA distances are more clustered in polymorph 2 than in polymorph 1.

Another way to assess the structural difference between these polymorphs is to compare their morphologies predicted by the BFDH model. This model predicts the anisotropic growth of crystals on the basis of the spacing between lattice planes. According to this model, the crystals of polymorph 1 grow more elongated than those of polymorph 2. This predicted difference is consistent with our limited observations that polymorph 1 forms needle-like crystals and polymorph 2 plate-like ones. By this comparison, the structure of polymorph 1 is more anisotropic than that of polymorph 2.

We next consider the differences in molecular conformation between the co-crystal polymorphs. For NIC, conformational flexibility is associated mainly with the torsion of the amide group relative to the pyridine ring ( $\theta_1$  in Scheme 1). In both polymorphs, the amide group is rotated out of the pyridine plane ( $\theta_1 \neq 0$  or  $180^\circ$ ) but in different directions (the signs of  $\theta_1$  are different; see Table 2). It is noteworthy that the NIC conformations in NIC-RMA co-crystals differ from that in the crystal of pure NIC, whose amide group is rotated nearly  $180^\circ$  relative to the molecules in the NIC-RMA co-crystals. According to Lemmerer et al.,<sup>19</sup> the conformer in the pure

**Table 2.** Torsional Angles of NIC-RMA Co-Crystals

NIC	polymorph 1	polymorph 2	pure NIC <sup>a</sup>
$\theta_1$ , deg	−143.0 (mol 1) −167.5 (mol 2)	151.6	23.1
RMA	polymorph 1	polymorph 2	pure RMA <sup>b</sup>
$\theta_2$ , deg	−103.3 (mol 1) −129.5 (mol 2)	−106.0	−120.8 (mol 1) −122.5 (mol 2)
$\theta_3$ , deg	138.0 (mol 1) 135.1 (mol 2)	104.8	149.2 (mol 1) 98.2 (mol 2)

<sup>a</sup>Retrieved from CSD (NICOAM02).  $\theta_1$  is defined in Scheme 1. <sup>b</sup>Calculated from the crystal structure of *S*-mandelic acid (FEGHAA) in CSD.<sup>24</sup>  $\theta_2$  and  $\theta_3$  are defined in Scheme 1.

NIC crystal is close to the global minimum of the conformational energy curve relative to amide torsion, and those in the NIC-RMA co-crystals are near a local minimum ca. 1 kcal/mol higher in energy. Lemmerer et al. surveyed the changes of NIC conformation as a result of co-crystallization with carboxylic acids.<sup>19</sup>

Conformational differences are also seen in the RMA molecule between the NIC-RMA polymorphs. Table 2 shows the relevant torsional angles  $\theta_2$  and  $\theta_3$  that define the RMA conformations (see Scheme 1). The change of torsional angle is especially pronounced in  $\theta_3$ . Note, however, that similar changes exist between the two symmetry-independent molecules in the crystal of pure RMA. (We drew the last conclusion from the structure of *S*-mandelic acid,<sup>24</sup> for the CSD has no entry for RMA.)

The two polymorphs have different networks of hydrogen bonds (Figure 3). In polymorph 1, two NIC molecules form an

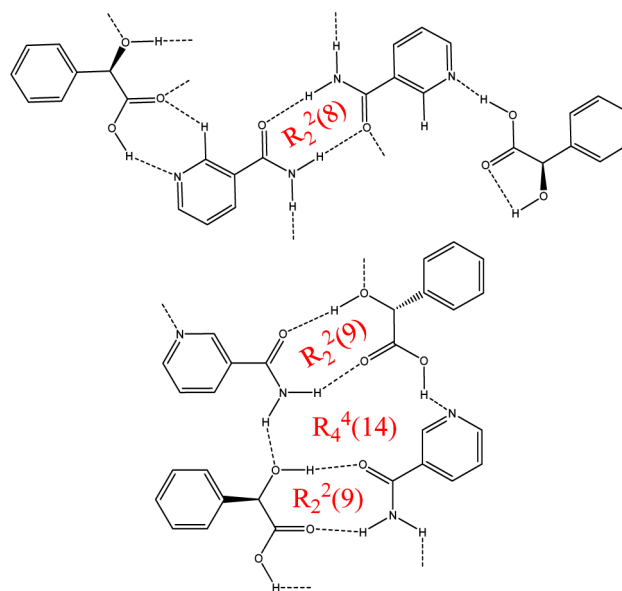


**Figure 3.** Hydrogen bonds in NIC-RMA co-crystal polymorph 1 (top) and polymorph 2 (bottom).

amide–amide  $R_2^2(8)$  “homo-dimer”, and RMA molecules are hydrogen-bonded to the NIC dimer through the carboxylic acid group of RMA and the pyridine N of NIC. In polymorph 2, NIC and RMA molecules hydrogen-bond to form  $R_2^2(9)$  “hetero-dimers” through the amide group of NIC and the  $\alpha$ -hydroxyl carbonyl group of RMA. These “hetero-dimers” are further joined by hydrogen bonds (carboxylic acid H···pyridine

N and hydroxyl O...amide anti-H; Figure 3, bottom) to form infinite ribbons along *b*.

The hydrogen-bonded  $R_2^2(9)$  "hetero-dimer" in polymorph 2 (Figure 3, bottom) is noteworthy in reference to the known structures of the co-crystals containing NIC and carboxylic acids. Of the 12 co-crystals formed by NIC and a monocarboxylic acid in the CSD, 9 have the NIC-NIC  $R_2^2(8)$  "homo-dimer" (including polymorph 1<sup>17</sup>), two have the  $R_2^2(8)$  "hetero-dimer" formed between the NIC amide group and the carboxylic acid group, and one does not have any dimer motif.<sup>19</sup> To our knowledge, the  $R_2^2(9)$  "hetero-dimer" in NIC-RMA polymorph 2 is not present in other co-crystals containing mandelic acid and an amide; for example, isonicotinamide,<sup>25</sup> piracetam,<sup>26</sup> (1*R*,3*S*)-camphoramic acid,<sup>27</sup> and NIC-RMA polymorph 1.

**Relative Stability of the Polymorphs of NIC-RMA Co-Crystals.** Figure 4a shows the typical DSC traces of the two polymorphs of NIC-RMA co-crystals ( $C_{AB1}$  and  $C_{AB2}$ ). Table 3 summarizes the relevant data from DSC measurements. Thermogravimetric analysis shows no significant weight loss for either polymorph up to 140 °C, indicating that the melting

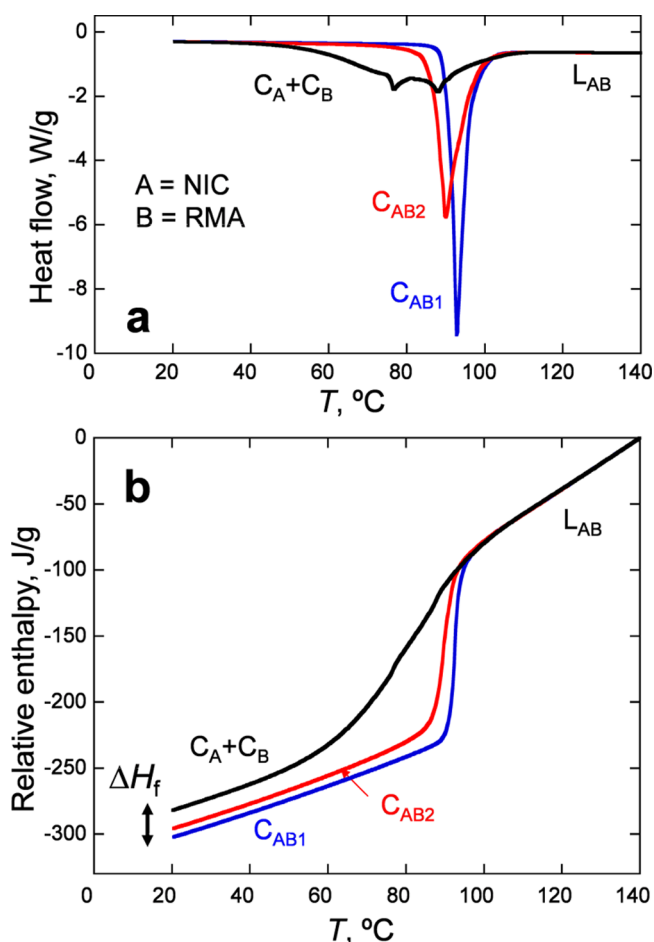


**Figure 4.** (a) DSC melting endotherms of the NIC-RMA co-crystals ( $C_{AB1}$  and  $C_{AB2}$ ) for the two polymorphs) and a physical mixture of the crystals of NIC and RMA at 1:1 molar ratio ( $C_A + C_B$ ). A and B refer to NIC and RMA, respectively. (b) Relative enthalpies of  $C_{AB1}$ ,  $C_{AB2}$ , and ( $C_A + C_B$ ) obtained by integrating the heat-flow data in (a) from the common liquid state of the three materials (starting from 140 °C). The enthalpy of a co-crystal relative to the physical mixture is its formation enthalpy  $\Delta H_f$ .

**Table 3.** Thermal Properties of NIC-RMA Polymorphs

phase	$T_m$ , °C	$\Delta H_m$ , J/g	$\Delta H_f$ , J/g	$T_g$ , °C
polymorph 1	89.1 (0.2) <sup>a</sup>	140.8 (0.4)	-23 (3)	-3.1 (0.1)
polymorph 2	85.2 (0.2)	128.4 (1.9)	-18 (3)	-4.2 (0.2)
$C_A$ (NIC)	128.3 (0.1)	197.0 (0.6)	0	<i>b</i>
$C_B$ (RMA)	131.7 (0.1)	176.9 (0.6)	0	<i>b</i>
$C_A + C_B$			0	-2.7 (0.1)

<sup>a</sup>Reference 17 reports 89 °C. <sup>b</sup> $T_g$  could not be measured due to crystallization.

data are uncorrupted by thermal decomposition. The  $T_g$  values in Table 3 are the glass transition temperatures observed during the second heating of the liquids produced by melting crystals. The similar  $T_g$  values indicate similar chemical compositions of the crystalline samples before melting.

Polymorph 1 is higher melting and has higher enthalpy of fusion than polymorph 2 (Table 3). The lower enthalpy of polymorph 1 is consistent with its higher density, a correlation observed for many polymorphic pairs.<sup>28</sup> According to the heat of fusion rule<sup>28</sup> and thermodynamic calculations,<sup>29</sup> the two polymorphs are monotropic, with polymorph 1 being more stable than polymorph 2 at any temperature. We tested this conclusion via polymorphic conversions. In the first experiment, a liquid of NIC and RMA at 1:1 molar ratio was formed between two coverslips and seeded with polymorphs 1 and 2 at opposite sides by contact with seed crystals. Both polymorphs grew into the liquid over time at room temperature. Viewed between crossed polarizers, crystals of polymorph 1 were gray and those of polymorph 2 were brighter and more colorful. The polymorphs were also distinguishable by X-ray diffraction and Raman microscopy. Polymorph 2 grew faster than polymorph 1; in some samples, polymorph 2 could be observed to grow along the interface between the melt and polymorph 1 (Figure 5a–c). This peculiar mode of crystal growth yielded samples useful for determining the relative stability of polymorphs 1 and 2. It is significant that after polymorph 2 covered the growth front of polymorph 1, the latter continued to grow in a different fiber-like morphology (Figure 5d). The fibers were confirmed to be polymorph 1 by Raman microscopy, and the surrounding crystals polymorph 2. Although the faster-growing polymorph 2 consumed most of the liquid, the subsequent conversion eventually transformed the sample to polymorph 1 in two months at 23 °C. This conversion indicates that polymorph 1 is more stable than polymorph 2.

In a second experiment to test the relative stability of polymorphs 1 and 2, solvent-mediated conversion was performed. Seeds of polymorph 1 (<1 mg) were added to a suspension of polymorph 2 (40 mg) in 0.2 mL of ACN. At 23 °C, polymorph 2 converted to polymorph 1 over time. Thus, observations of polymorphic conversion in both the solid state and in liquid suspension indicate that polymorph 1 is more stable than polymorph 2 near the ambient temperature. This finding and the higher melting point and higher heat of fusion of polymorph 1 are consistent with the prediction that the two polymorphs are monotropic.

**Formation Enthalpies of NIC-RMA Co-Crystals.** To obtain the formation enthalpies of NIC-RMA co-crystals, we measured the enthalpy changes for melting the co-crystals and the physical mixture of the component crystals (eq 2). For this purpose, the heat-flow data in Figure 4a were integrated from a common liquid-state temperature (140 °C) down to a common solid-state temperature (20 °C). The results are shown in

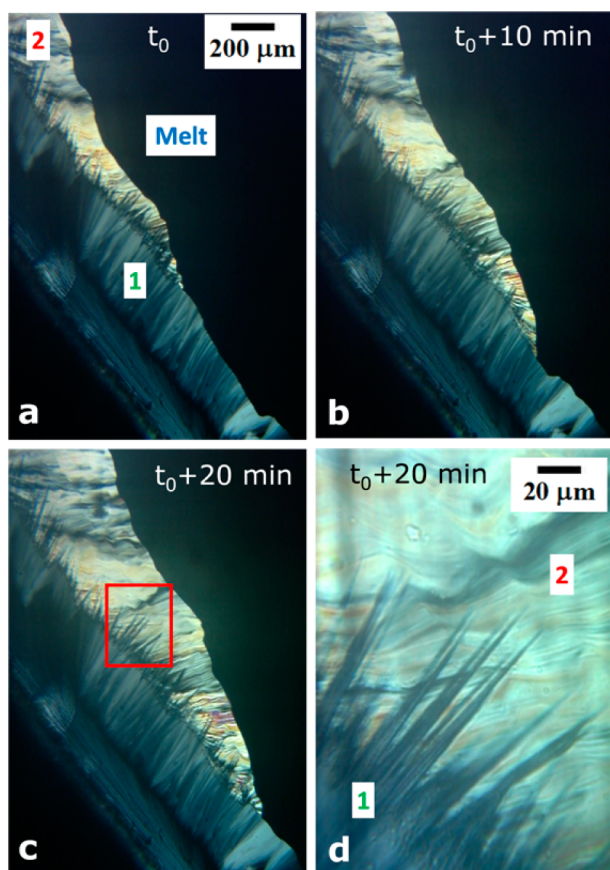


**Figure 5.** (a–c) Simultaneous growth and transformation of NIC-RMA co-crystal polymorphs 1 (1) and 2 (2). The same scale bar applies to (a–c). (d) Enlarged view of the box in (c).

Figure 4b. The enthalpies of the co-crystals relative to the physical mixture are their formation enthalpies. NIC being polymorphic,<sup>23</sup> the physical mixture of NIC and RMA was prepared to contain the stable NIC polymorph (CSD: NICOAM02), in accord with the thermodynamic convention for evaluating formation enthalpies. Both co-crystal polymorphs have lower enthalpies than the physical mixture of component crystals:  $\Delta H_f = -23$  (3) J/g for polymorph 1 and  $-18$  (3) J/g for polymorph 2. These values are consistent with those reported for several co-crystals that contain saccharin.<sup>9</sup>

Figure 4a shows that upon heating, the physical mixture ( $C_A + C_B$ ) undergoes several thermal events en route to the liquid state. These events could involve formation of co-crystals, eutectic melting, and dissolution. It is noteworthy, however, that the exact sequence of events is immaterial for our purpose of determining the enthalpy of melting the physical mixture, so long as the heat flow is integrated from the initial temperature at which ( $C_A + C_B$ ) is solid ( $T_s$ ) to the final temperature at which the mixture is liquid ( $T_l$ ). This conclusion follows the path independence in calculating enthalpy changes. While calorimetric error can increase when integrating over a wide temperature range, such concerns diminish with the improved baseline stability and precision of modern DSCs and can be assessed objectively from the reproducibility of data.

The slopes of the liquid and solid portions in Figure 4b are the respective heat capacities reported by the DSC instrument (TA Instruments Q2000) operating in the standard mode. The instrument is capable of more accurate determination of heat capacities, but we made no effort to do so because for the

purpose of determining  $\Delta H_f$ , a constant shift of heat capacity only rotates the set of curves in Figure 4b and does not change the  $\Delta H_f$  values.

For our method to be valid, the physical mixture of component crystals must not react to form co-crystals before DSC analysis. Such stability was confirmed for all the physical mixtures by XRD prior to DSC. The significantly different DSC traces of the physical mixtures from those of the co-crystals (Figure 4a) also indicate no substantial transformation to co-crystals. Finally, consecutive measurements of the same physical mixture showed no significant changes of melting enthalpies, again suggesting the mixture was stable.

DSC measurements were performed to measure the enthalpy of mixing the liquids of NIC and RMA,  $\Delta H_{mix}$ . We did so to assess whether it is necessary to correct for nonideal mixing in calculating formation enthalpies of co-crystals via thermodynamic cycles and, in particular, whether measurements are needed with the physical mixture of component crystals as opposed to the pure component crystals. Figure 6a shows the

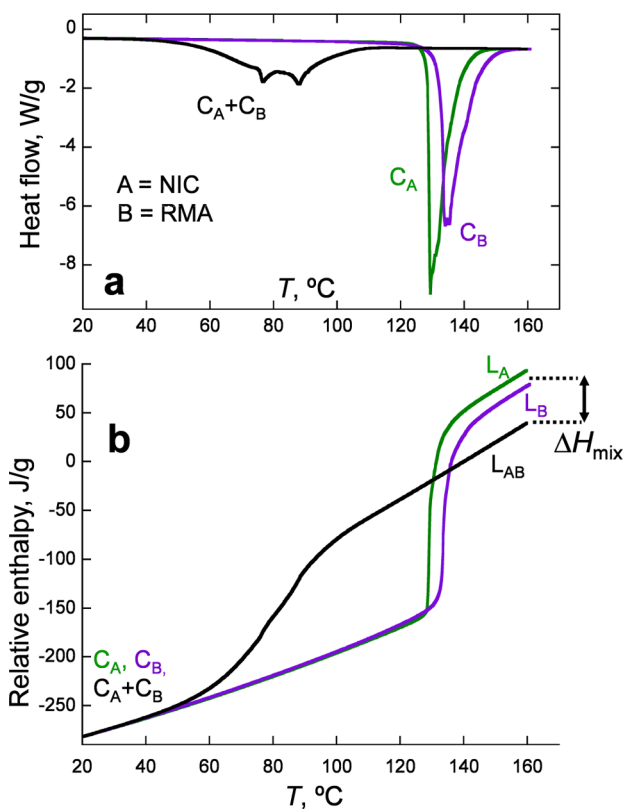


**Figure 6.** (a) DSC melting endotherms of NIC crystals ( $C_A$ ), RMA crystals ( $C_B$ ), and their physical mixture at 1:1 molar ratio. (b) Relative enthalpies of liquid NIC ( $L_A$ ), liquid RMA ( $L_B$ ), and their solution  $L_{AB}$  obtained by integrating the heat-flow data in (a) from 20 °C. The enthalpy of mixing NIC and RMA liquids is the enthalpy of  $L_{AB}$  relative to the average enthalpy of the component liquids ( $L_A$  and  $L_B$ ) weighted according to the 1:1 molar ratio.

melting endotherms of the crystals of NIC, the crystals of RMA, and their physical mixture at 1:1 molar ratio. Because physically mixing NIC and RMA crystals is expected to have negligible change in enthalpy, the enthalpy of mixing for NIC and RMA liquids can be obtained by integrating the three endotherms in Figure 6a from a common solid-state temperature (20 °C) to a common liquid-state temperature (160 °C).

If  $\Delta H_{\text{mix}} = 0$ , the enthalpy of the NIC-RMA solution ( $L_{\text{AB}}$  in Figure 6b) would lie between those of the pure liquids ( $L_{\text{A}}$  and  $L_{\text{B}}$ ). In contrast,  $L_{\text{AB}}$  is substantially below  $L_{\text{A}}$  and  $L_{\text{B}}$ . Our data yield  $\Delta H_{\text{mix}} = -49$  (4) J/g for mixing liquid NIC and RMA at 160 °C at 1:1 molar ratio.

The significant enthalpy of mixing for liquid NIC and RMA makes it necessary to account for this effect in calculating their co-crystals' formation enthalpies via thermodynamic cycles. In other words, eqs 2 and 3 are preferred over eqs 4 and 5, unless the latter are modified as by Oliveira et al. to account for nonideal mixing.<sup>9</sup> Without correction for nonideal mixing, our data in Figures 5 and 6 would lead to *positive* formation enthalpies for the NIC-RMA co-crystals.

It is of interest to compare the enthalpy of formation for a co-crystal  $\Delta H_{\text{f}}$  and the enthalpy of mixing for the liquid components  $\Delta H_{\text{mix}}$ .  $\Delta H_{\text{f}}$  is the enthalpy change for the solid-state reaction  $C_{\text{A}} + C_{\text{B}} = C_{\text{AB}}$  (eq 1);  $\Delta H_{\text{mix}}$  is the enthalpy change for the liquid-state reaction  $L_{\text{A}} + L_{\text{B}} = L_{\text{AB}}$ . For the NIC-RMA system,  $\Delta H_{\text{f}}$  and  $\Delta H_{\text{mix}}$  are both negative (reactions are exothermic), indicating the mixed state has lower energy than the separated state. For this system,  $\Delta H_{\text{f}}$  is approximately half  $\Delta H_{\text{mix}}$ , although we note that the two values were measured at different temperatures (30 and 160 °C). Work is in progress to measure liquid heat capacities to obtain  $\Delta H_{\text{mix}}$  at the same temperature at which  $\Delta H_{\text{f}}$  is measured. It might be instructive to systematically compare  $\Delta H_{\text{f}}$  and  $\Delta H_{\text{mix}}$  for co-crystallizing systems to learn the extent to which the stability of a co-crystal is ascribable to favorable enthalpy of mixing in the liquid state. To this end, the method described here may prove useful for collecting data on both  $\Delta H_{\text{f}}$  and  $\Delta H_{\text{mix}}$ .

## CONCLUSION

Co-crystals provide an opportunity to improve solid-state properties for pharmaceuticals and other materials. We have studied the co-crystallization of nicotinamide (NIC) and R-mandelic acid (RMA), a member of the class of co-crystals containing NIC and carboxylic acids. We report a new polymorph of the NIC-RMA co-crystal and propose a procedure for determining the formation enthalpies of co-crystals. In this procedure, enthalpy changes are measured for the melting (or dissolution) of a co-crystal and the physical mixture of its component crystals. Because the two processes arrive at the same liquid, the difference of their enthalpy changes is the co-crystal's formation enthalpy. For NIC-RMA co-crystals, the error in calculated formation enthalpies is substantial from neglecting nonideal mixing in the liquid state, and the error is likely significant for other co-crystal systems and must be taken into account in calculating their formation enthalpies via thermodynamic cycles.

In our calorimetric method, the enthalpy changes are measured for the transformation of a co-crystal and a physical mixture of component crystals to the same physical state. The use of a physical mixture of component crystals, as opposed to the pure component crystals, automatically corrects for nonideal mixing in the liquid state in calculating the co-crystal's formation enthalpy. While we have implemented the method with a temperature-scanning calorimeter to measure heats of melting (eq 2), one can do so with an isothermal calorimeter to acquire heats of solution (eq 3). Regardless of its implementation, this method has the potential of providing thermodynamic data for understanding the stability and prediction of co-crystals. For example, the data can be used to validate computer models for calculating the formation

energies of co-crystals and to extract empirical structure–energy relations.

In future studies, it would be of interest to apply the calorimetry method to series of co-crystals in which the components are systematically varied. By doing so, one can probe the molecular factors that influence the formation and stability of co-crystals. Also valuable would be a systematic comparison of the enthalpies of co-crystal formation and the enthalpies of liquid-state mixing, both quantities readily obtained using our method, to learn whether the thermodynamics of liquid mixing can help understand the stability of co-crystals. Finally, it is desirable to determine the free energies of formation of co-crystals, which requires that the entropy effect be included:  $G = H - TS$ . Such efforts would extend to general co-crystal systems the methods for measuring free-energy differences between racemic compounds and conglomerates of resolvable enantiomers.<sup>30,31</sup> The free energies of formation define the thermodynamic stability of co-crystals relative to their component crystals and manufacturing conditions under which co-crystals are favored. In advancing the science of co-crystals, thermodynamic studies are a valuable complement to structural and kinetic investigations.

## ASSOCIATED CONTENT

### Supporting Information

The crystallographic data on NIC-RMA polymorph 2 are included (PDF and CIF). This material is available free of charge via the Internet at <http://pubs.acs.org>.

## AUTHOR INFORMATION

### Corresponding Author

\*E-mail: [lyu@pharmacy.wisc.edu](mailto:lyu@pharmacy.wisc.edu).

### Notes

The authors declare no competing financial interest.

## ACKNOWLEDGMENTS

We thank Pfizer and the National Science Foundation (DMR 0804786) for supporting this work and Paul Meenan and Brendan Murphy for helpful discussions.

## REFERENCES

- (1) Findlay, A.; Campbell, A. N.; Smith, N. O. *Phase Rule and Its Applications*; Dover Publications: Mineola, NY, 1951.
- (2) Jacques, J.; Collet, A.; Wilen, S. H. *Enantiomers, Racemates, and Resolutions*; Krieger Publishing Company: Malabar, FL, 1991.
- (3) Almarsson, Ö.; Zaworotko, M. J. *Chem. Commun.* **2004**, 1889–1896.
- (4) Vishweshwar, P.; McMahon, J. A.; Bis, J. A.; Zaworotko, M. J. *J. Pharm. Sci.* **2006**, *95*, 499–516.
- (5) Good, D. J.; Rodríguez-Hornedo, N. *Cryst. Growth Des.* **2009**, *9*, 2252–2264.
- (6) McNamara, D. P.; Childs, S. L.; Giordano, J.; Iarriccio, A.; Cassidy, J.; Shet, M. S.; Mannion, R.; O'Donnell, E.; Park, A. *Pharm. Res.* **2006**, *23*, 1888–1897.
- (7) Li, Z. B.; Yang, B. S.; Jiang, M.; Eriksson, M.; Spinelli, E.; Yee, N.; Senanayake, C. *Org. Process Res. Dev.* **2009**, *13*, 1307–1314.
- (8) Chatteraj, S.; Shi, L.; Sun, C. C. *CrystEngComm* **2010**, *12*, 2466–2472.
- (9) Oliveira, M. A.; Peterson, M. L.; Davey, R. J. *Cryst. Growth Des.* **2011**, *11*, 449–457.
- (10) Chadha, R.; Saini, A.; Arora, P.; Jain, D. S.; Dasgupta, A.; Row, T. N. G. *CrystEngComm* **2011**, *13*, 6271–6284.

- (11) Vishweshwar, P.; McMahon, J. A.; Peterson, M. L.; Hickey, M. B.; Shattocka, T. R.; Zaworotko, M. J. *Chem. Commun.* **2005**, 4601–4603.
- (12) Ueto, T.; Takata, N.; Muroyama, N.; Nedu, A.; Sasaki, A.; Tanida, S.; Terada, K. *Cryst. Growth Des.* **2011**, *12*, 485–494.
- (13) Porter, W. W.; Elie, S. C.; Matzger, A. J. *Cryst. Growth Des.* **2008**, *8*, 14–16.
- (14) Braga, D.; Palladino, G.; Polito, M.; Rubini, K.; Grepioni, F.; Chierotti, M. R.; Gobetto, R. *Chem.—Eur. J.* **2008**, *14*, 10149–10159.
- (15) Gryl, M.; Krawczuk, A.; Stadnicka, K. *Acta Crystallogr., Sect. B: Struct. Sci.* **2008**, *64*, 623–632.
- (16) Aitipamula, S.; Chow, P. S.; Tan, R. B. H. *CrystEngComm* **2009**, *11*, 1823–1827.
- (17) Frišćić, T.; Jones, W. *Faraday Discuss.* **2007**, *136*, 167–178.
- (18) Rasool, A. A.; Hussain, A. A.; Ditter, L. W. *J. Pharm. Sci.* **1991**, *80*, 387–393.
- (19) Lemmerer, A.; Esterhuysen, C.; Bernstein, J. *J. Pharm. Sci.* **2010**, *99*, 4054–4071.
- (20) Berry, D. J.; Seaton, C. C.; Clegg, W.; Harrington, R. W.; Coles, S. J.; Horton, P. N.; Hursthouse, M. B.; Storey, R.; Jones, W.; Frišćić, T.; Blagden, N. *Cryst. Growth Des.* **2008**, *8*, 1697–1712.
- (21) Fleischman, S. G.; Kuduva, S. S.; McMahon, J. A.; Moulton, B.; Walsh, R. D. B.; Rodriguez-Hornedo, N.; Zaworotko, M. J. *Cryst. Growth Des.* **2003**, *3*, 909–919.
- (22) Braun, D. E.; Ardid-Candel, M.; D’Oria, E.; Karamertzanis, P. G.; Arlin, J.-B.; Florence, A. J.; Jones, A. G.; Price, S. L. *Cryst. Growth Des.* **2011**, *11*, 5659–5669.
- (23) Li, J.; Bourne, S. A.; Caira, M. R. *Chem. Commun.* **2011**, *47*, 1530–1532.
- (24) Patil, A. O.; Pennington, W. T.; Paul, I. C.; Curtin, D. Y.; Dykstra, C. E. *J. Am. Chem. Soc.* **1987**, *109*, 1529–1535.
- (25) Aakeroy, C. B.; Beatty, A. M.; Helfrich, B. A. *J. Am. Chem. Soc.* **2002**, *124*, 14425–14432.
- (26) Viertelhaus, M.; Hilfiker, R.; Blatter, F.; Neuburger, M. *Cryst. Growth Des.* **2009**, *9*, 2220–2228.
- (27) Hu, Z. Q.; Nie, J. J.; Xu, D. J.; Xu, Y. Z.; Chen, C. L. *J. Chem. Crystallogr.* **2001**, *31*, 109–113.
- (28) Burger, A.; Ramberger, R. *Mikrochim. Acta* **1979**, *2*, 259–271.
- Burger, A.; Ramberger, R. *Microchim. Acta* **1979**, *2*, 273–316.
- (29) Yu, L. *J. Pharm. Sci.* **1995**, *84*, 966–974.
- (30) Reutzel-Edens, S. M.; Russell, V. A.; Yu, L. *J. Chem. Soc., Perkin Trans. 2* **2000**, *5*, 913–924.
- (31) Yu, L.; Huang, J.; Jones, K. J. *J. Phys. Chem. B* **2005**, *109*, 19915–19922.